Desalination and Water Treatment
www.deswater.com
doi: 10.1080/19443994.2016.1141712

57 (2016) 23864–23872
October

Taylor & Francis
Taylor & Francis Group

A novel way to prepare pyrrhotite and its performance on removal of phosphate from aqueous solution

Tianhu Chen[a,*], Yadan Shi[a], Haibo Liu[a], Dong Chen[a], Ping Li[a], Yan Yang[b], Xiao Zhu[a]

[a] *Laboratory for Nanomineralogy and Environmental Material, School of Resources & Environmental Engineering, Hefei University of Technology, Hefei, China, Tel. +86 13956099615, +86 0551 2903990; emails: chentianhu@hfut.edu.cn (T. Chen), 270587723@qq.com (Y. Shi), liuhaibosky116@hfut.edu.cn (H. Liu), cdxman@hfut.edu.cn (D. Chen), 344753438@qq.com (P. Li), 867434719@qq.com (X. Zhu)*

[b] *Civil Engineering, College of Engineering and Informatics, National University of Ireland, Galway, Ireland, email: y.yang1@nuigalway.i.e.*

Received 6 July 2015; Accepted 22 December 2015

ABSTRACT

Adsorbent is a key factor influencing the removal of phosphate from aqueous solution in terms of adsorption technique. In this present work, limonite-pyrrhotite (L-pyr) was prepared by the reaction of natural limonite with sulfur derived from the decomposition of pyrite. The L-pyr was utilized to remove phosphate from aqueous solution. The effect of preparation temperature, initial *P* concentration, initial solution pH, oxygen amount, and interference ions on the *P* removal was investigated to evaluate the performance of L-pyr. The results showed that increased oxygen amount favored the phosphate removal and the effect of solution pH can be ignored as the initial solution pH was not more than 8.5. The existence of NO_3^- improved phosphate removal in contrast with the negative role of Cl^-, SO_4^{2-}, and HCO_3^- in an order: $HCO_3^- > SO_4^{2-} > Cl^-$. As for kinetic study, the adsorption onto L-pyr can be fitted well to pseudo-second-order model. The experimental results provided a novel way to prepare L-pyr having an effective performance in the removal of phosphate and easy to be separated from aqueous solution by means of magnetic separation technique.

Keywords: Pyrite; Pyrrhotite; Limonite; Phosphorus removal; Magnetic separation

---

1. Introduction

It is necessary to remove phosphate from sewage before discharging into natural environments because phosphorus is a key factor to eutrophication. In the past decades, adsorption technique has been documented as an effective method to remove phosphate from aqueous solution [1,2]. Moreover, adsorption method possessed several advantages as compared with the biological technology and chemical technology due to low cost, high selectivity, and high capacity [3–5].

As for adsorption technique, the key factor influencing the removal of phosphate was the adsorbent. Therefore, the development and utilization of novel adsorbents have attracted extensive attention. Up to now, adsorbents for the removal of phosphate from aqueous solution were mainly focused on clay minerals [3,4,6–9], metal oxides [5,10–13], and solid wastes

---

*Corresponding author.

[14–16]. Of these adsorbents, the performance of natural mineral materials and solid wastes on the removal of phosphate attracted more and more attention, not only for developing novel and effective adsorbent, but also for the sufficient utilization of resources, such as montmorillonite, zeolite, kaolinite, and low-grade iron ore. To improve the performance of materials, material sometimes was treated by modification before using. For instance, the report of Kasama et al. indicated that montmorillonite, beidellite, saponite, and fluor-tetrasilicic expandable mica pillared with Keggin ion-like Al clusters increased the adsorption capacities to 20.5, 24.5, 25.1, and 27.0 mg P/g, respectively, in contrast to undetectable phosphate adsorption capacities onto their parent clay minerals [17]. Tian et al. reported that the pillared montmorillonite by La/Al remarkably increased the adsorption capacity of the parent clay [18]. Still, the limonite treated at a high temperature (550℃) in hydrogen also significantly enhanced the phosphate removal [19]. On the other hand, pyrite utilized as an important raw material for preparing sulfuric acid was rarely reported as a kind of adsorbent. In our group, pyrite was used to prepare pyrrhotite for removal of heavy metal ions (Cu^{2+}, Pb^{2+}, Cd^{2+}, Zn^{2+}) and recycling the Cu in the Cu-rich wastewater by flowing column experiments [20,21].

According to the study on pyrite, limonite-pyrrhotite (L-pyr) was prepared by the reaction of sulfur with limonite, where sulfur was derived from the decomposition of pyrite. Moreover, the performance of L-pyr on the removal of phosphate was investigated and compared with the pyrrhotite (pyr) derived from the decomposition of pyrite. The objective of this study was to explore the utilization of pyrite and limonite to prepare an environmentally friendly adsorbent and to investigate its performance on the removal of phosphate from aqueous solution. Therefore, the effect of relative parameters (initial P concentration, initial solution pH, oxygen amount, interference ions, etc.) on the removal of phosphate was carried out.

2. Experimental

2.1. Material preparation

Natural limonite and pyrite were obtained from Tongling city, Anhui province, China. Both samples were crushed and screened into a size lower than 75 μm. The pyrite and limonite were put into a quartz tube. The former was put into the under-part and the latter was put into the above-part, where silica wool was put into the middle of both samples. A kind of inert gas (argon) was utilized to drive the air away from the bottom before annealing. After the designed time, both samples were collected for further characterization after cooling down in argon. The sample obtained from the reaction of limonite with sulfur was labeled as L-pyr and the sample derived from the decomposition of pyrite was labeled as Pyr. L-pyr-650 means this L-pyr was obtained from the reaction of limonite and sulfur at 650℃.

2.2. Characterization

X-ray diffraction (XRD) of raw samples and annealed samples was measured using a Rigaku powder diffractometer with Cu Kα radiation. The tube voltage was 40 kV, and the current was 100 mA. The XRD diffraction patterns were taken in the range of 20–70° at a scan speed of 4 min^{-1}. Phase identification was carried out by comparison with those included in the Joint Committee of Powder Diffraction Standards database.

Magnetic susceptibility of samples was measured using a susceptibility meter (Bartington MS2).

The X-ray photoelectron spectroscopy (XPS) measurements were carried out to analyze the surface of L-pyr-650 before and after adsorption of phosphate using a Thermo ESCALAB 250 XI system equipped with monochromatic Al Kα source.

2.3. Batch experiments

In this work, batch experiments were carried out to evaluate the performance of this L-pyr and the effect of relative parameters (initial P concentration, coexistence ions, etc.).

Phosphorus(P)-containing sewage was prepared by dissolving KH_2PO_4 in deionized water with a resistivity of 18.4 MΩ cm. Firstly, the effect of annealing temperature was evaluated by adsorption of 5 mg/L of PO_4^{3-}-P using different L-pyr prepared at different reaction temperatures under the fixed conditions: contact time 24 h, dosages 200 mg, and liquid volume 100 mL. In addition, the performance of L-pyr-650 on the removal of phosphate was also evaluated at different solution pHs (3.5, 5, 6.5, 7.5, 8.5, 9.5, 11.5, and 12).

Secondly, the effect of initial concentration of phosphate on the removal of phosphate from aqueous solution by L-pyr-650 was investigated under the fixed conditions: initial concentration (2, 5, and 10 mg/L), L-pyr-650 200 mg, and liquid volume 100 mL. In addition, the performance of L-pyr-650 was compared with the Pyr.

Thirdly, the effect of the interference and ion strength on the P removal was undertaken by addition of four types of anions (Cl^-, NO_3^-, SO_4^{2-}, HCO_3^-) with different concentrations (0.01, 0.05, 0.1, 0.5, and 1, 2 mol/L) under the fixed condition: 5 mg PO_4^{3-}-P/L, L-pyr-650 50 mg, liquid volume 100 mL, and pH 6.3. Meanwhile, the effect of oxygen amount and contact temperature was also assessed under the condition.

Finally, kinetic analysis was carried out in this section under different initial *P* concentrations, different oxygen amounts, and different initial solution pHs according to the pseudo-second-order kinetic model.

In the whole experiment, the phosphate in the supernatant solution was extracted after the desired experimental time followed by filtration (0.22-μm film) and was measured by the method proposed by Murphy and Riley [22]. The phosphate removal was calculated from the decreases of phosphate concentrations relative to those of the initial concentrations.

3. Results and discussion

3.1. Characterization

The result of XRF indicated the limonite was mainly composed of Fe_2O_3 58.85 wt%, SiO_2 16.87 wt%, Al_2O_3 4.85 wt%, MnO 3.16 wt%, CaO 1.05 wt%, ZnO 1.6 wt%, others 2.4 wt%, and the loss on ignition 11.22 wt%. In addition, the XRD patterns of L-pyr obtained from the reaction at different temperatures are presented in Fig. 1. The reflections at $2\theta = 21.2$, 33.3, 36.8, 41.3, 53.3° were found and identified as goethite (α-FeOOH). The reflection at $2\theta = 26.4°$ was identified as quartz. Therefore, it was confirmed that the limonite mainly contained goethite and quartz.

As displayed in Fig. 1, all the reflections of goethite disappeared after reaction at 500℃ and were replaced by that of hematite ascribed to the Eq. (1). As the temperature reached to 550℃, the new reflections were observed and identified as magnetite. The formation of magnetite contributed to the Eq. (2). As the temperature came to 570℃, the new reflections at $2\theta = 34.1$, 44, and 53.4° were found and identified as pyrrhotite. The formation of pyrrhotite was ascribed to the Eq. (3). When the temperature reached to 650℃, only the reflection of pyrrhotite remained. That is to say, the goethite was completely transformed into pyrrhotite in the presence of sulfur as the reaction temperature was not lower than 650℃.

$$FeOOH \rightarrow Fe_2O_3 + H_2O \tag{1}$$

$$Fe_2O_3 + S \rightarrow Fe_3O_4 + SO_2 \tag{2}$$

$$Fe_3O_4 + S \rightarrow FeS + SO_2 \tag{3}$$

On the other hand, the magnetic susceptibility also confirmed the transformation process. As displayed in Fig. 2, the magnetic susceptibility experienced a remarkable increase to $6{,}812 \times 10^{-8}\ m^3\ kg^{-1}$ and then decreased to $700 \times 10^{-8}\ m^3\ kg^{-1}$. This change tendency was dependent on the ratio between magnetite (Fe_3O_4) and pyrrhotite (FeS). The more the magnetite was, the higher the magnetic susceptibility was. Therefore, it can be concluded that the hematite was completely transformed into magnetite in the presence of sulfur after reaction at 550℃ having the maximum magnetic susceptibility. As the temperature varied from 550 to 700℃, the magnetite was transformed gradually into pyrrhotite resulting in the decrease of the magnetic

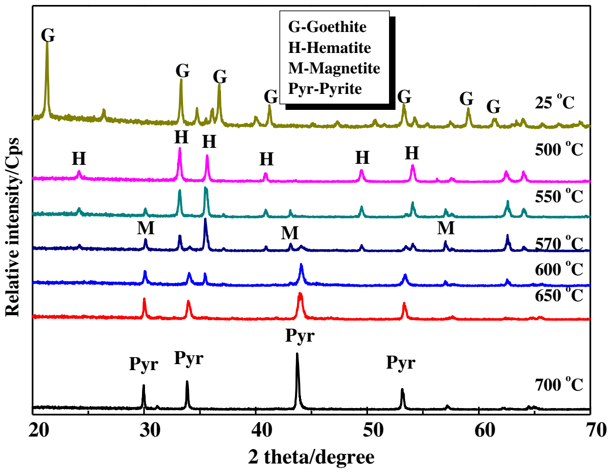

Fig. 1. XRD patterns of limonite and reacted products at different reaction temperatures.

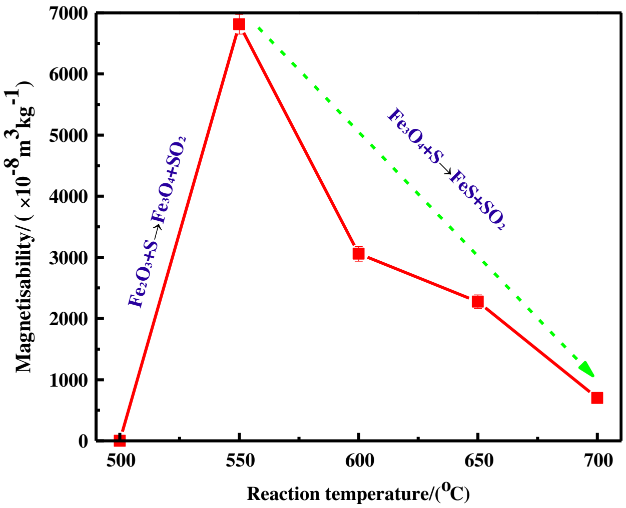

Fig. 2. Magnetic susceptibility of the reacted products at different temperatures.

susceptibility. Even so, this material obtained from the reaction not lower than 550°C still can be separated from the aqueous solution easily by means of magnetic separation technique (the figure not shown here).

3.2. Effect of reaction temperature

As discussed above, the reaction temperature affected the composition of the reacted products. Properties of the different products differed with each other probably resulting in the difference of the adsorption performance. Therefore, the effect of preparation temperature of the pyrrhotite on the *P* removal was investigated and the results were shown in Fig. 3. The *P* removal increased to 99.9% from 35% and then decreased to 52% as the temperature increased to 800°C from 400°C. And the phosphate was almost removed (99.9%) as the annealing temperature was 650 and 700°C. It indicated that the newly formed magnetite improved the removal of phosphate from aqueous solution. Compared with the magnetite, the newly formed L-pyr displayed a better performance on adsorption of phosphate. As the initial *P* concentration was 5 mg/L, the L-pyr derived from the reaction of Fe_3O_4 with *S* can remove almost all phosphate from the aqueous solution as presented in Fig. 3. However, as the annealing temperature increased to 800°C, the phosphate removal experienced a dramatic decrease by 47.9%. The transformation of hematite into magnetite enhanced the surficial activity to form adsorption sites (–OH by protonation and Fe^{3+} by oxidation of Fe^{2+}), which increased the *P* removal. The increased annealing temperature (650 or 700°C) favored the formation of pyrite which considerably improved the removal of phosphate, implying that the L-pyr had a better surficial activity to adsorb phosphate. The surficial activity should be contributed to the easy oxidation of L-pyr forming more adsorption sites. However, the crystallization of L-pyr increased the crystal size and decreased the surface area leading to the decrease in the surficial reactivity and decreasing the *P* removal.

3.3. Effect of initial PO_4^{3-} concentration

The difference of Pyr and L-pyr-650 on the removal of phosphate and the effect of initial *P* concentration on the *P* removal were displayed in Fig. 4. Obviously, the *P* removal over L-pyr was always higher than that over Pyr in the experimental period. It indicated the L-pyr had a better performance on adsorption of phosphate than that of Pyr. The result agreed well with the previous report that the SG-pyr (SG-synthetic goethite) had a better *P* removal than Pyr [23]. On the other hand, the initial *P* concentration also affected the removal of phosphate. In particular, the *P* removal increased to 41.5% as the contact time increased to 28 h and the initial *P* concentration was 10 mg/L. However, the *P* removal reached to 99.9% in the first 2 and 24 h as the initial *P* concentration was 2 and 5 mg/L, respectively. Undoubtedly, the increased *P* concentration enhanced the competition of phosphate for the adsorption sites. Therefore, the increased *P* concentration reduced the *P* removal in

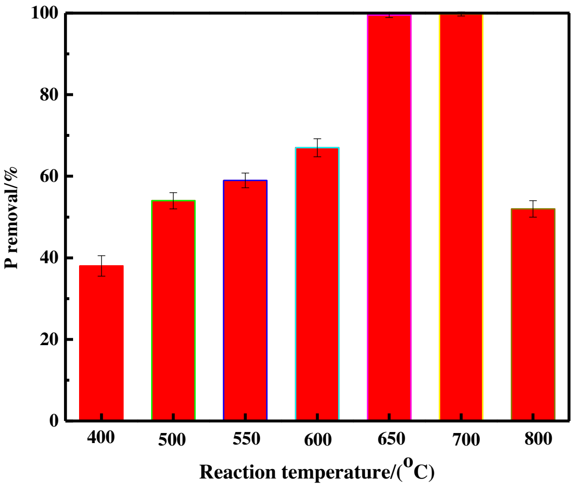

Fig. 3. The effect of different L-pyr prepared at different reaction temperatures on the *P* removal (experimental conditions: initial *P* concentration 5 mg/L, liquid volume 100 mL, pH 6.9 ± 0.1, L-pyr 200 mg).

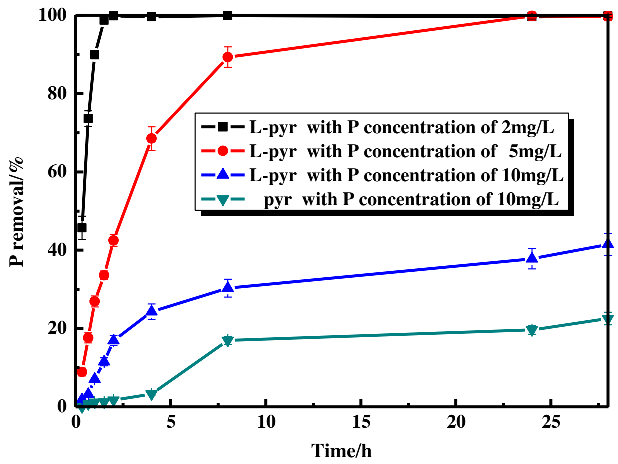

Fig. 4. The effect of Pyr and L-pyr-650 as well as the initial *P* concentration (experimental conditions: liquid volume 100 mL, pH 6.9 ± 0.1, L-pyr-650 200 mg).

the experimental period, although the prolonged time favored the increase in the *P* removal.

3.4. Effect of initial solution pH

As well known, solution pH significantly influenced the surficial activity of adsorbents. To make the effect of solution pH on the *P* removal clear, the initial solution pH (3.5, 5, 6.5, 7.5, 8.5, 9.5, 11.5, and 12) was designed and the results were presented in Fig. 5. As seen in Fig. 5, the *P* removal increased to 99.9% in the first 1.5 h as the initial solution pH was not less than 7.5. The time for the complete removal of phosphate increased to 4 and 8 h when the initial solution pH was 8.5 and 9.5, respectively. As the initial solution pH increased to 11.5 and 12, the highest *P* removal just reached to 78.4 and 61.2%, respectively, despite adsorbing 24 h. It indicated that this material had a good performance as the initial solution pH was not more than 8.5. The result was not consistent with the previous report that the acidic condition suppressed the oxidation of Fe^{2+} into Fe^{3+} leading to the decrease in the *P* removal [24]. In contrast, the lower the pH was, the better the *P* removal was in this present work. This phenomenon was relative with the point of zero charge of FeS which was determined as 6.3 in this work. Therefore, as the solution pH was lower than 6.3, the surface of FeS presented positive charge, which favored the adsorption of phosphate with a negative charge. Inversely, the increasing solution pH inhibited the surface adsorption by electrostatic interaction. On the other hand, As the initial solution pH was over 9.5, although the condition was a benefit to the oxidation of Fe^{2+}, it also favored the formation of $Fe(OH)_3$ [25]. Therefore, the hydroxyl group competed Fe^{3+} with PO_4^{3-} [26], which resulted in the decrease of *P* removal at high pH.

3.5. Interference study

The interference of various ions and the effect of their concentration on the *P* removal were investigated. The fixed experimental conditions were as followed: dosage 200 mg, initial *P* concentration 5 mg/L, liquid volume 100 mL, pH 6.9 ± 0.1, and adsorption time 24 h.

As displayed in Fig. 6, the *P* removal increased to 94.2% from 77.3% as the concentration of NO_3^- increased to 2 M from 0.01 M. Compared with the absence of extra ions, the presence of NO_3^- favored the removal of phosphate as shown in Fig. 6. However, as the NO_3^- was replaced by Cl^-, SO_4^{2-}, or HCO_3^-, the *P* removal experienced a decrease at different degrees. The *P* removal decreased to 64.4, 52.1, and 7.4% for Cl^-, SO_4^{2-}, and HCO_3^-, respectively, as the concentration of the coexistence ion increased to 2 M. It indicated that the existence of Cl^-, SO_4^{2-}, or HCO_3^- hindered the removal of phosphate and the order of the negative role was $HCO_3^- > SO_4^{2-} > Cl^-$. To the best of our knowledge, NO_3^- was able to accelerate the corrosion of iron forming iron oxides and mean-

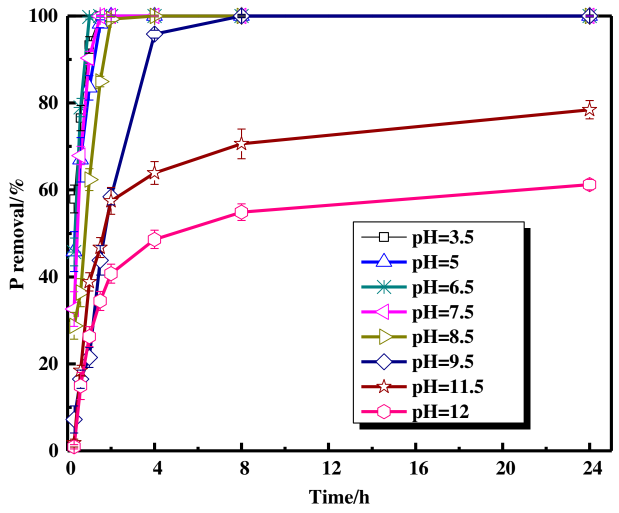

Fig. 5. The effect of initial solution pH on the removal of phosphate by L-pyr-650 (experimental conditions: initial *P* concentration 5 mg/L, liquid volume 100 mL, L-pyr-650 200 mg).

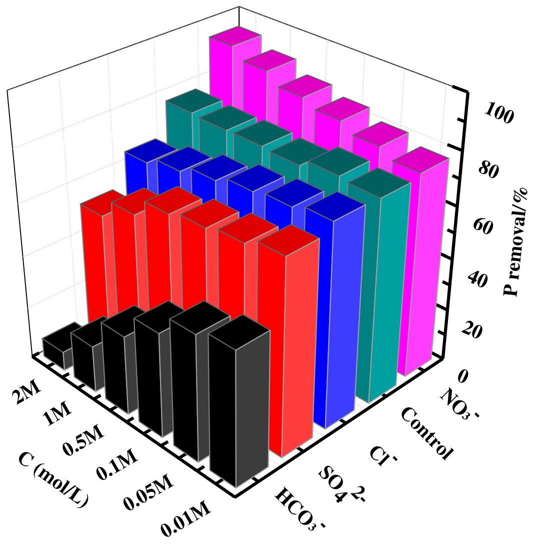

Fig. 6. The effect of interference ions and corresponding ion concentration on the *P* removal by L-pyr-650 (experimental conditions: initial *P* concentration 5 mg/L, liquid volume 100 mL, L-pyr-650 200 mg, pH 6.9 ± 0.1).

while NO_3^- could be reduced into NO_2^-, N_2, and NH_4^+ [27]. Therefore, it was speculated the existence of NO_3^- favored the oxidation of L-pyr forming much more Fe^{3+}. And the increasing concentration of NO_3^- also enhanced the oxidation process of L-pyr resulting in the increase in the *P* removal with increasing NO_3^- concentration. The affinity of HCO_3^- to the corrosion products of iron has been reported extensively and the competition of HCO_3^- with other anions for the adsorption sites was also reported. For example, the existence of HCO_3^- remarkably inhibited the removal of arsenate by zero-valent iron. Therefore, it is supposed the HCO_3^- compete the adsorption sites with phosphate which led to the decrease in the *P* removal. As for SO_4^{2-}, it was reported that the presence of SO_4^{2-} accelerated the corrosion of iron and promoted the formation of green rust ($GR(SO_4^{2-})$) [28]. However, the sulfur in the iron sulfide was mainly oxidized into SO_4^{2-}. Thereby, the addition of SO_4^{2-} likely hindered the oxidation of L-pyr playing a negative role in the removal of phosphate.

To the best of our knowledge, no report on the effect of Cl^- on the *P* removal by pyrrhotite can be found. On the other hand, the effect of Cl^- on the surficial reactivity of iron in aqueous solution has been reported extensively. However, the role of Cl^- in the corrosion of FeO seems to be a controversy. The increased Cl^- concentration from 0.02 to 3 mM decreased the corrosion rate of iron [29]. However, the study of Ruangchainikon et al. indicated that the presence of Cl^- favored the formation of green rust (GR (Cl^-)), promoting the performance of FeO [30]. Therefore, in the present work, it was speculated that the restriction efficiency of Cl^- was higher than the promotion efficiency due to the formation of GR(Cl^-) as the concentration of Cl^- was between 0.01 and 2 M, although the green rust was demonstrated to be a good material for the removal of phosphate [31]. However, the presence of green rust remarkably favored the increase in the *P* removal as the concentration of Cl^- was not less than 0.2 mM.

3.6. Effect of oxygen amount

The effect of oxygen amount on the *P* removal was shown in Fig. 7. Oxic means the conical beaker was exposed in air; anoxic means the conical beaker was sealed in the adsorption process; and anaerobic means oxygen in the conical beaker was driven away followed by the addition of adsorbent. These conditions denoted different oxygen amounts in the adsorption system. As seen in Fig. 7, the *P* removal experienced a dramatic increase to 99.9% in the oxic condition. Meanwhile, the *P* removal just increased to 45.1 and 27.6% in the anoxic and anaerobic condition, respectively. The results showed that increased oxygen amount in the adsorption system favored the removal of phosphate from aqueous solution. This phenomenon was caused by the role of dissolved oxygen in the formation of Fe^{3+} by the oxidation of L-pyr-60. Adequate oxygen can ensure the oxidation of L-pyr-60 into Fe^{3+} followed by the formation of Fe-P precipitant. This result agreed well with the previous reports that adequate oxygen amount improved the removal of phosphate by FeO and Fe^{2+} [19,24]. That is to say, the removal of phosphate by FeO or Fe^{2+} considerably depended on their oxidation rate and subsequent formation of Fe-P precipitant. And the oxygen amount was adequate to oxidize Fe^0 or Fe^{2+} so long as the adsorption system was exposed in air. The explanation also can be used in this work. Therefore, the adequate oxygen improved the removal of phosphate.

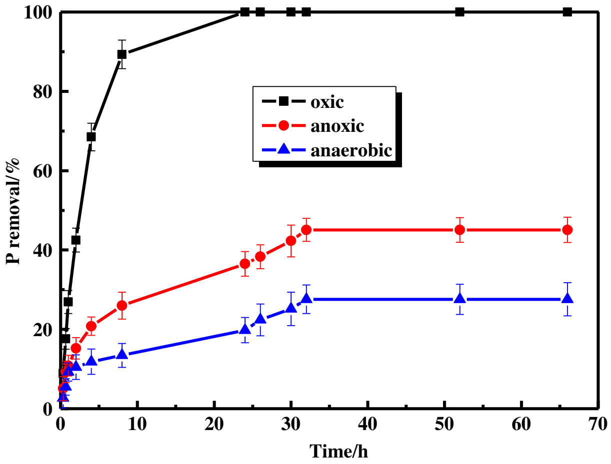

Fig. 7. The effect of oxygen amount on the *P* removal (experimental conditions: initial *P* concentration 5 mg/L, liquid volume 100 mL, pH 6.9 ± 0.1, L-pyr-650 200 mg. The oxic system denotes the adsorption process is exposed to air. The anoxic system denotes the adsorption process is closed in a tube, and anaerobic system denotes the adsorption process is closed in a tube and the dissolved oxygen is driven away by boiling).

On the other hand, the P-adsorbed L-pyr-650 under different oxygen conditions was characterized by XPS. As displayed in Fig. 8, a peak width between 132.4 and 135.6 eV can be observed and was attributed to the binding energy of PO_4^{3-}. The peak at 133.9 eV should be ascribed to the combination between Fe^{3+} and phosphate [32,33]. The XPS analysis showed that the peak of PO_4^{3-} binding energy can be observed clearly after adsorption in the oxic condition. However, no obvious peak can be found for the anoxic and anaerobic condition. It implied that much more *P* was detected on the surface of the L-pyr-650 in the oxic

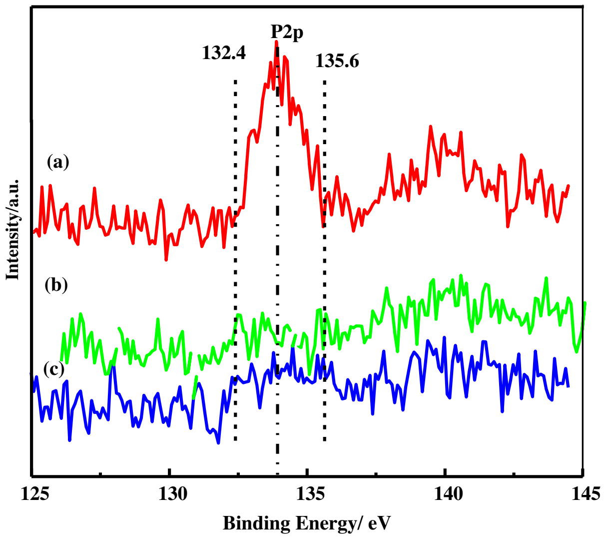

Fig. 8. XPS of the P-adsorbed L-pyr-650 under different conditions after adsorption for 24 h: oxic (a), anaerobic (b), and anoxic (c).

condition as compared with the anoxic and anaerobic condition. As mentioned above, the oxic condition remarkably favored the removal of phosphate from aqueous solution. Thereby, the results of XPS also confirmed the phenomenon.

3.7. Effect of adsorption temperature

As presented in Fig. 9, contact temperature obviously affected the *P* removal. The increasing temperature increased the *P* removal as the adsorption time was lower than 20 h, although phosphate can be removed completely after 30 h at the experimental temperature. As discussed above, the removal of phosphate depended on the oxidation rate of L-pyr. Therefore, it was proposed that the increase in contact temperature favored the oxidation of L-pyr-650 increasing the adsorption sites which enhanced the adsorption performance. Thereby, the high temperature favored the removal of phosphate from aqueous solution by L-pyr-650.

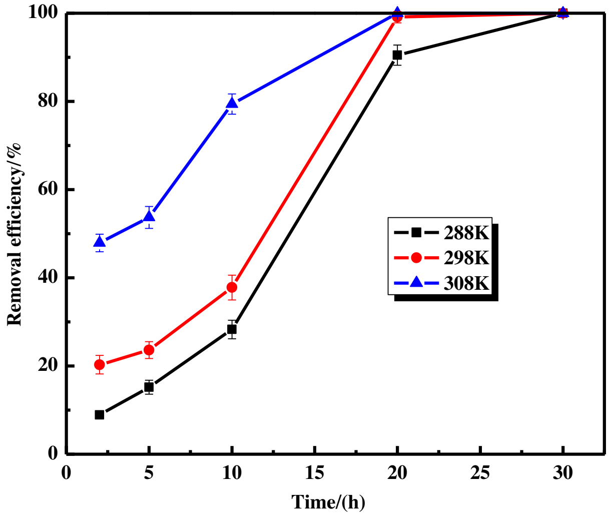

Fig. 9. The effect of contact temperature on the *P* removal by L-pyr-650 (experimental conditions: initial *P* concentration 5 mg/L, liquid volume 100 mL, L-pyr-650 200 mg, pH 6.9 ± 0.1).

3.8. Kinetic studies

The pseudo-second-order kinetic equation [34] as followed was utilized to describe the kinetic data of L-pyr adsorption phosphate, $t/q_t = 1/kq_e^2 + t/q_e$, where t (min) is adsorption time, q_t and q_e (mg/g) are adsorption amount at the time of t and equilibrium, respectively, and k is rate constant. As displayed in

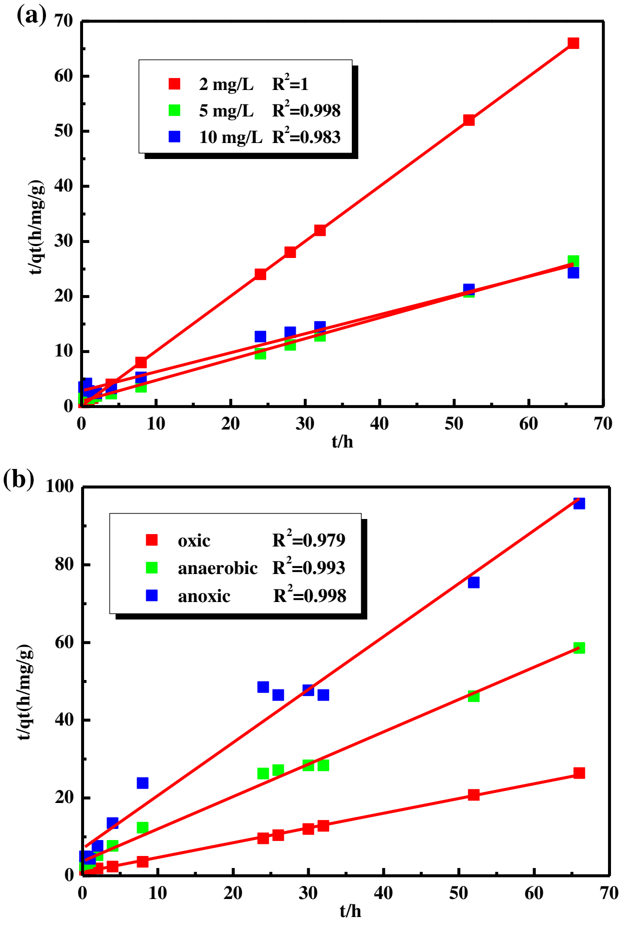

Fig. 10. Linear plot of pseudo-second-order model for adsorption phosphate by L-pyr at different conditions: different initial *P* concentration (a), oxygen amount (b), and different initial pH (c).

Fig. 10, according to the experimental results of the effect of initial P concentration, oxygen amount, and initial pH on the P removal, the relations between t/q_t and t were plotted. The results indicated t/q_t had a good linear relationship with t and the value of correlation coefficient (R^2) was over 0.97, especially for the effect of initial solution pH (over 0.998). As seen in Fig. 10, it can be speculated from the slope of the straight line that the low initial P concentration, high oxygen amount, and low solution pH had a quick adsorption rate. It indicated that high oxygen amount and low solution pH favored the removal of phosphate from aqueous solution. This fitted kinetic result was agreed well with the results of batch experiment.

4. Conclusions

L-pyr can be prepared by the reaction of limonite with sulfur which is derived from the decomposition of pyrite. The newly formed L-pyr had a great performance on the removal of phosphate especially after annealing at 650 and 700℃. As the initial solution pH was not more than 8.5, L-pyr-650 could remove almost all of the phosphate from the aqueous solution as the initial P concentration was not more than 5 mg/L. Moreover, the oxic condition remarkably enhanced the performance of L-pyr-650. As for interference ions, the existence of NO_3^- favored the removal of phosphate in contrast to the passive role of Cl^-, HCO_3^-, and SO_4^{2-} in an order of $HCO_3^- > SO_4^{2-} > Cl^-$. Finally, the increase in temperature also improved the removal of phosphate. In addition, this material was also proved to be easy to separate from aqueous solution by magnetic separation technique. These experimental results provided important information on the preparation of pyrrhotite and its application in the removal of phosphate. Most importantly, the results demonstrated that L-pyr was a kind of promising adsorbent for treatment of P-containing wastewater and could be separated from aqueous solution easily by magnetic separation technique.

Acknowledgments

The authors acknowledge the support of the projects of the Natural Science Foundation of China (No. 41402030, 41402029).

References

[1] S.L. Daniels, D.G. Parker, Removing phosphorus from waste water, Environ. Sci. Technol. 7 (1973) 690–694.
[2] N. Bellier, F. Chazarenc, Y. Comeau, Phosphorus removal from wastewater by mineral apatite, Water Res. 40 (2006) 2965–2971.
[3] W. Huang, J. Chen, F. He, J. Tang, D. Li, Y. Zhu, Y. Zhang, Effective phosphate adsorption by Zr/Al-pillared montmorillonite: Insight into equilibrium, kinetics and thermodynamics, Appl. Clay Sci. 104 (2015) 252–260.
[4] S. Wei, W. Tan, F. Liu, W. Zhao, L. Weng, Surface properties and phosphate adsorption of binary systems containing goethite and kaolinite, Geoderma 213 (2014) 478–484.
[5] G. Li, S. Gao, G. Zhang, X. Zhang, Enhanced adsorption of phosphate from aqueous solution by nanostructured iron(III)–copper(II) binary oxides, Chem. Eng. J. 235 (2014) 124–131.
[6] L. Deng, Z. Shi, Synthesis and characterization of a novel Mg–Al hydrotalcite-loaded kaolin clay and its adsorption properties for phosphate in aqueous solution, J. Alloys Compd. 637 (2015) 188–196.
[7] G. Li, D. Chen, W. Zhao, X. Zhang, Efficient adsorption behavior of phosphate on La-modified tourmaline, J. Environ. Chem. Eng. 3 (2015) 515–522.
[8] M. Yang, J. Lin, Y. Zhan, H. Zhang, Adsorption of phosphate from water on lake sediments amended with zirconium-modified zeolites in batch mode, Ecol. Eng. 71 (2014) 223–233.
[9] Z. Chen, Q. Jin, Z. Guo, G. Montavon, W. Wu, Surface complexation modeling of Eu(III) and phosphate on Na-bentonite: Binary and ternary adsorption systems, Chem. Eng. J. 256 (2014) 61–68.
[10] H. Wang, J. Zhu, Q.-L. Fu, J.-W. Xiong, C. Hong, H.-Q. Hu, A. Violante, Adsorption of phosphate onto ferrihydrite and ferrihydrite-humic acid complexes, Pedosphere 25 (2015) 405–414.
[11] I. Perassi, L. Borgnino, Adsorption and surface precipitation of phosphate onto $CaCO_3$–montmorillonite: Effect of pH, ionic strength and competition with humic acid, Geoderma 232–234 (2014) 600–608.
[12] Q. Yu, Y. Zheng, Y. Wang, L. Shen, H. Wang, Y. Zheng, N. He, Q. Li, Highly selective adsorption of phosphate by pyromellitic acid intercalated ZnAl-LDHs: Assembling hydrogen bond acceptor sites, Chem. Eng. J. 260 (2015) 809–817.
[13] Y. Su, H. Cui, Q. Li, S. Gao, J.K. Shang, Strong adsorption of phosphate by amorphous zirconium oxide nanoparticles, Water Res. 47 (2013) 5018–5026.
[14] P.R. Rout, P. Bhunia, R.R. Dash, Modeling isotherms, kinetics and understanding the mechanism of phosphate adsorption onto a solid waste: Ground burnt patties, J. Environ. Chem. Eng. 2 (2014) 1331–1342.
[15] X. Yuan, C. Bai, W. Xia, J. An, Acid-base properties and surface complexation modeling of phosphate anion adsorption by wasted low grade iron ore with high phosphorus, J. Colloid Interface Sci. 428 (2014) 208–213.
[16] T.E. Köse, B. Kıvanç, Adsorption of phosphate from aqueous solutions using calcined waste eggshell, Chem. Eng. J. 178 (2011) 34–39.
[17] T. Kasama, Y. Watanabe, H. Yamada, T. Murakami, Sorption of phosphates on Al-pillared smectites and mica at acidic to neutral pH, Appl. Clay Sci. 25 (2004) 167–177.
[18] S. Tian, P. Jiang, P. Ning, Y. Su, Enhanced adsorption removal of phosphate from water by mixed lanthanum/aluminum pillared montmorillonite, Chem. Eng. J. 151 (2009) 141–148.

[19] H. Liu, T. Chen, X. Zou, Q. Xie, C. Qing, D. Chen, R.L. Frost, Removal of phosphorus using NZVI derived from reducing natural goethite, Chem. Eng. J. 234 (2013) 80–87.

[20] Y. Yang, T. Chen, P. Li, H. Liu, J. Xie, Q. Xie, X. Zhan, Removal and recovery of Cu and Pb from single-metal and Cu–Pb–Cd–Zn multimetal solutions by modified pyrite: Fixed-bed columns, Ind. Eng. Chem. Res. 53 (2014) 18180–18188.

[21] T. Chen, Y. Yang, P. Li, H. Liu, J. Xie, Q. Xie, X. Zhan, Performance and characterization of calcined colloidal pyrite used for copper removal from aqueous solutions in a fixed bed column, Int. J. Miner. Process. 130 (2014) 82–87.

[22] J. Murphy, J.P. Riley, A modified single solution method for the determination of phosphate in natural waters, Anal. Chim. Acta 27 (1962) 31–36.

[23] X. Zhu, T. Chen, L. Yan, H. Liu, P. Li, X. Zou, Phase evolution and performance characteristic of pyrite-goethite anaerobic roasting product, J. Chin. Ceram. Soc. 42 (2014) 1435–1440.

[24] T. Li, H. Wang, W. Dong, T. Liu, F. Ouyang, Q. Zhang, Phosphate removal during Fe(II) oxidation in the presence of Cu(II): Characteristics and application for electro-plating wastewater treatment, Sep. Purif. Technol. 132 (2014) 388–395.

[25] B. Morgan, O. Lahav, The effect of pH on the kinetics of spontaneous Fe(II) oxidation by O_2 in aqueous solution–basic principles and a simple heuristic description, Chemosphere 68 (2007) 2080–2084.

[26] L. Lijklema, Interaction of orthophosphate with iron (III) and aluminum hydroxides, Environ. Sci. Technol. 14 (1980) 537–541.

[27] H.B. Liu, T.H. Chen, D.Y. Chang, D. Chen, Y. Liu, H.P. He, P. Yuan, R. Frost, Nitrate reduction over nanoscale zero-valent iron prepared by hydrogen reduction of goethite, Mater. Chem. Phys. 133 (2012) 205–211.

[28] J. Gui, T.M. Devine, The influence of sulfate ions on the surface enhanced raman spectra of passive films formed on iron, Corros. Sci. 36 (1994) 441–462.

[29] E.J. Reardon, Anaerobic corrosion of granular iron: Measurement and interpretation of hydrogen evolution rates, Environ. Sci. Technol. 29 (1995) 2936–2945.

[30] C. Ruangchainikom, C.H. Liao, J. Anotai, M.T. Lee, Effects of water characteristics on nitrate reduction by the Fe^0/CO_2 process, Chemosphere 63 (2006) 335–343.

[31] K. Barthélémy, S. Naille, C. Despas, C. Ruby, M. Mallet, Carbonated ferric green rust as a new material for efficient phosphate removal, J. Colloid Interface Sci. 384 (2012) 121–127.

[32] R. Franke, T. Chassé, P. Streubel, A. Meisel, Auger parameters and relaxation energies of phosphorus in solid compounds, J. Electron. Spectrosc. Relat. Phenom. 56 (1991) 381–388.

[33] W.F. Stickle, J.F. Moulder, P.E. Sobol, Handbook of X-ray Photoelectron Spectroscopy, Perkin-elmer Corporation Publisher, Montreal, 2004.

[34] L. Lei, X. Li, X. Zhang, Ammonium removal from aqueous solutions using microwave-treated natural Chinese zeolite, Sep. Purif. Technol. 58 (2008) 359–366.